13th World Conference on Earthquake Engineering
Vancouver, B.C., Canada
August 1-6, 2004
Paper No. 768

EARTHQUAKE SOURCE GEOMETRY COMPATIBLE WITH STRONG MOTION DATA

R.N.Iyengar[1] and S.T.G.Raghukanth[2]

SUMMARY

Empirical random process models, based only on past data, are in vogue for simulating strong motion accelerograms. These are used to evaluate the safety of important structures like large dams and nuclear power plants. However, to make the results more rational one has to incorporate source mechanics into these models. The acceptability of such results depends on how realistically the source zone, several kilometers below the surface, can be modeled. The source zone of a strong earthquake can be mapped indirectly, if several reliable surface level strong motion records are available for an earthquake event. Since earthquakes are rare, such data does not accrue fast, making data acquisition costly. This is all the more a reason why available data should be put to optimal use to understand the type of ground motion that may arise in future. With this in view, several ensembles of past strong motion records have been analyzed in this paper to identify and map the causative zone of the corresponding events. The region encompassing the strong motion accelerograph (SMA) array is modeled as a layered elastic half space with known properties. The source is represented as a sequence of double couples evolving as ramp functions, triggering at different instants, distributed in a region yet to be mapped. The known surface level ground motion time histories are treated as responses to the unknown double couples on the fault surface. The location, orientation, magnitude and rise time of the double couples are found by minimizing the mean square error between the analytical and recorded solutions. Suitable constraints are used to arrive at physically meaningful solutions. Numerical results are presented for San Fernando, Imperial Valley, Uttarakashi, and Chi-Chi earthquakes. Results obtained are in good agreement with those obtained from other approaches.

INTRODUCTION

Success of earthquake resistant design practice critically depends on how correctly the future seismic ground motion, arising out of potential faults, can be estimated at a site. At present engineers heavily rely on empirical approaches to estimate ground motion through attenuation relations and response spectral shapes. Such an approach presupposes that the hazard to the built environment is mainly from ground vibration with no ground failure during or at the end of the event. This may be reasonable when the site is

[1] Professor, Dept. of Civil Engineering, Indian Institute of Science, Bangalore 560012,India.
E-mail : rni@civil.iisc.ernet.in
[2] Research Fellow, Indian Institute of Science, Bangalore 560012, India, E-mail : rk@civil.iisc.ernet.in

far away from the source, or when the causative fault does not run underneath an inhabited city. However, there have been examples in the recent past where structural failure could be attributed to near source motion leading to severe ground deformation. Engineering codes generally advise that sites susceptible for ground failure should be avoided [1]. While this is sound advice for new constructions, existing cities and heritage sites still pose a challenge. In this context, analytical estimation of surface level ground motion from source mechanism models will be superior to empirical methods of hazard estimation. Among the different seismological source formulations, the double couple model is perhaps the most appealing from a physical point of view. Previously in the literature, this has been discussed by Aki [2] and Haskell [3]. Bouchon [4, 5], Deodatis *et al* [6] and Zhang *et al* [7] have demonstrated that surface level ground motions can be computed for a horizontally layered medium with a buried double couple. It is noted that, once a realistic source is specified, finding the near source ground motion is a matter of detailed computations. However, limitations in such an approach arise due to inadequacies in demarcating the source geometry and the spatial variability of the slip. Even under the assumption of zero volume expansion [8], the fault interface need not be a smooth planar surface. Inversion of recorded data for finding source parameters has been carried out mainly in two ways. In the first, hypocenter location, duration and focal mechanism are found from teleseismic records assuming a point source model. In the other, near-field strong motion records are used to infer the slip distribution in space and time on an extended source. The point model derived from teleseismic data provides a basic picture of the source mechanism but is not sufficiently appealing to be used for computing ground motion in engineering problems. The near source motion is largely affected by the spatial and temporal variability of the fault slip. To address this issue there have been efforts in the past to delineate the source by inverting strong motion records [9,10,11,12,13]. In these approaches, the main fault location and orientation is assumed to be known on the basis of teleseismic information and aftershock distribution. The fault plane is divided into smaller subfaults of equal area and the evolution of the slip is assumed to be like a ramp function. The slip amplitude, rupture time and rise time are found by inverting the strong motion data. Introduction of physically meaningful constraints help the computations to converge towards acceptable results. Das and Suhaldoc [14] have studied the effect of various such constraints in source determination. Inversion of recorded data is a subtle exercise, possibly leading to non-unique solutions. If the problem is to simulate possible ground motion records at a site due to a known active fault, the details of which are buried, one needs to incorporate uncertainties arising due to possible nonplanar nature of the fault surface. The source model should have the potential to handle variabilities in slip values. The model for the region should be able to reflect variation in the velocity structure and quality facotrs. As a step in this direction, one will have to find for past earthquakes the source location, geometry and other parameters using only near source data. With this in the background a method is presented here to determine the details of a SMA compatible, siesmologically consistent source model, which is an improvement over the model previously presented by Iyengar and Agarwal [15]. It is demonstrated that strong motion data can be directly used to arrive at a compatible source description by modeling the region as a layered elastic halfspace. Numerical results are presented for San Fernando-1971, Imperial Valley-1979, Uttarkashi-1991, and Chi-Chi-1999 earthquakes.

DATA

Strong motion records are generally available in terms of accelerations. However, due to computational difficulties associated with high frequencies, velocity records sampled uniformly at a time step of 0.1s, are used here for further work. These can be obtained by integrating available SMA data from the global database (http://peer.berkeley.edu/smcat/). Four events with SMA data in the near source region are selected for analysis. The Imperial Valley (M_w=6.6) and San Fernando (M_w=6.4) earthquakes are from USA. The Uttarakashi (M_w=6.8) earthquake is from India and the Chi-Chi (M_w=7.6) earthquake is from Taiwan. These are selected keeping in view the availability of sufficient number of SMA records in the near source region. In all the four cases, reliable results from other approaches are available for evaluating the present model. For the Imperial Valley and Chi-Chi events the triggering times of the stations, which are networked together, are available. For the other two events starting times of the records are not known. For such data, a compatible set of starting times among the stations in the array needs to be found out, before proceeding further.

ANALYSIS

The rupture of the fault surface during an earthquake can be visualized as a series of dislocations [8]. The seismologically consistent force generated during the event on the fault surface can be modeled as a family of double couples applied at different time instants.

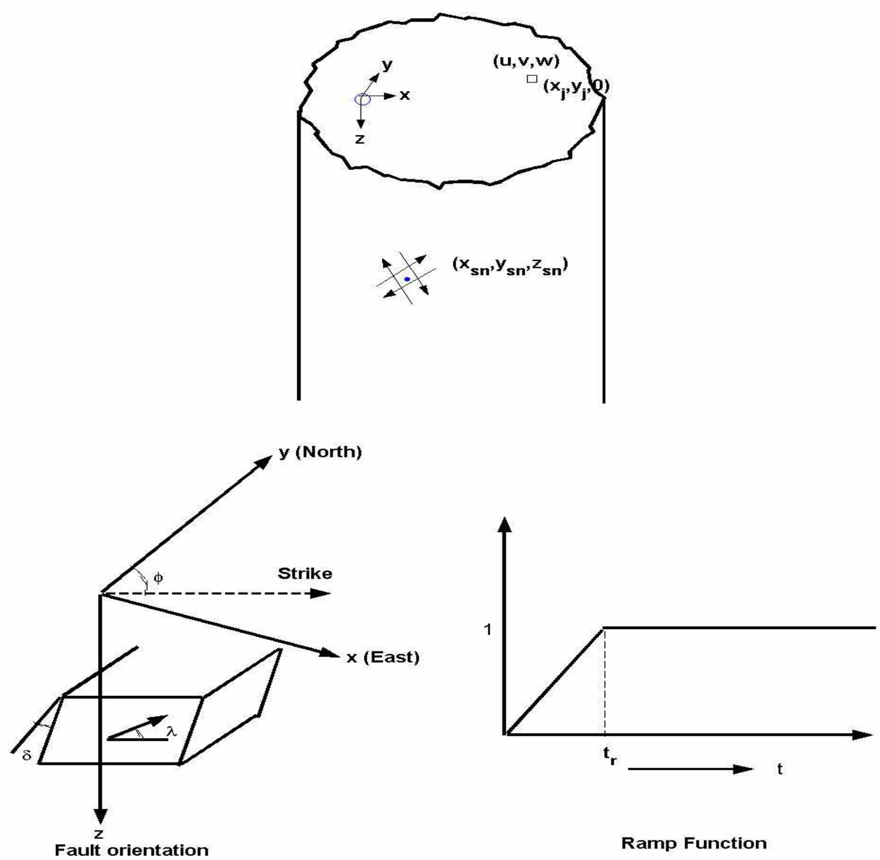

Figure 1. Seismic Source Mechanism and Related Terminology

With reference to Figure 1 the surface velocity $(\dot{u}_j, \dot{v}_j, \dot{w}_j)$ at a point $(x_j,y_j,0)$ on the surface of a homogeneous half-space, excited by a unit double couple acting at (x_s,y_s,z_s) is given by

$$\dot{u}\,(x_j,y_j,0,t) = \int\int\int_{-\infty}^{\infty} i\omega\, \tilde{m}(\omega)\, \tilde{G}_x(\kappa_x,\kappa_y,\omega,x_s,y_s,z_s,\phi,\lambda,\delta)\, \exp(-i\kappa_x x_j - i\kappa_y y_j - i\omega t)\, d\kappa_x d\kappa_y d\omega = C_{x,jn}$$

$$\dot{v}\,(x_j,y_j,0,t) = \int\int\int_{-\infty}^{\infty} i\omega\, \tilde{m}(\omega)\, \tilde{G}_y(\kappa_x,\kappa_y,\omega,x_s,y_s,z_s,\phi,\lambda,\delta)\, \exp(-i\kappa_x x_j - i\kappa_y y_j - i\omega t)\, d\kappa_x d\kappa_y d\omega = C_{y,jn}$$

$$\dot{w}\,(x_j,y_j,0,t) = \int\int\int_{-\infty}^{\infty} i\omega\, \tilde{m}(\omega)\, \tilde{G}_z(\kappa_x,\kappa_y,\omega,x_s,y_s,z_s,\phi,\lambda,\delta)\, \exp(-i\kappa_x x_j - i\kappa_y y_j - i\omega t)\, d\kappa_x d\kappa_y d\omega = C_{z,jn} \quad (1)$$

Here (k_x, k_y) and ω refer to the spatial and temporal frequencies respectively. The source time function is taken as a ramp function with $\tilde{m}(\omega)$ as its Fourier transform. The rupture surface is approximated as consisting of discrete planar dislocations, with location (x_{sn},y_{sn},z_{sn}) and orientation $(\phi_n, \delta_n, \lambda_n)$. $(\tilde{G}_x, \tilde{G}_y, \tilde{G}_z)$ are complex functions representing the frequency-wave number spectra of the region in terms of P- and S-wave velocities and damping factor Q. The elasto-dynamic analysis of a layered half-space subjected to a double couple source is available in the literature [6,7] and hence further details are not presented here. Ground motion during an earthquake may be thought of as being generated by a sequence of such double couples triggering at equal intervals of time Δt. For a sequence of double couples acting at the location $(x_{sn},y_{sn},z_{sn}$, n=1,2,..N) the velocity response at station j with coordinates $(x_j,y_j,0)$ will be of the form,

$$\begin{aligned}\dot{u}_j(t) &= \sum_{n=1}^{N} M_n C_{x,jn}\\ \dot{v}_j(t) &= \sum_{n=1}^{N} M_n C_{y,jn}\\ \dot{w}_j(t) &= \sum_{n=1}^{N} M_n C_{z,jn}\end{aligned} \tag{2}$$

Here, M_n stands for the unknown moment value. The problem of finding a compatible source reduces to the determination of $(M_n,t_{rn},\phi_n,\delta_n,\lambda_n,x_{sn},y_{sn},z_{sn})$ such that they are compatible with the station records $(\dot{u}_j, \dot{v}_j, \dot{w}_j)$. Strong motion instruments are self-triggered at a low level of ground acceleration when the initial velocity may be taken as zero. But the relative starting time of member stations within an array will not be known, unless the instruments are networked to trigger together. As the rupture initiates at a depth, the stations should be responding sequentially depending on their respective distance from the source region. For older SMA data available in the literature this time sequencing is not known. This demands preprocessing of the velocity data set for arriving at a compatible set of starting times for the records. Let, τ_j be the starting time for the j^{th} station, with respect to the initiation of rupture at the focus. If, a point source is assumed as a preliminary model, it follows that a single double couple M_0 will be acting at the focus (x_0,y_0,z_0) with orientation $(\phi_0,\delta_0,\lambda_0)$. From equations (1) it follows, at station j the velocity response will be

$$\begin{aligned}\dot{u}_j(t-\tau_j) &= M_0 C_{x,j0}\\ \dot{v}_j(t-\tau_j) &= M_0 C_{y,j0}\\ \dot{w}_j(t-\tau_j) &= M_0 C_{z,j0}\end{aligned} \tag{3}$$

Now, taking Fourier transform one gets in frequency domain

$$\begin{aligned}\tilde{\dot{u}}_j e^{-i\omega\tau_j} &= M_0 \tilde{C}_{x,j0}\\ \tilde{\dot{v}}_j e^{-i\omega\tau_j} &= M_0 \tilde{C}_{y,j0}\\ \tilde{\dot{w}}_j e^{-i\omega\tau_j} &= M_0 \tilde{C}_{z,j0}\end{aligned} \tag{4}$$

These equations will not be precisely satisfied leading to the total mean square error function

$$\varepsilon^2 = \sum_{j=1}^{M} \int_0^\infty [(\tilde{\dot{u}}_j e^{-i\omega\tau_j} - M_0 \tilde{C}_{x,j0})^2 + (\tilde{\dot{v}}_j e^{-i\omega\tau_j} - M_0 \tilde{C}_{y,j0})^2 + (\tilde{\dot{w}}_j e^{-i\omega\tau_j} - M_0 \tilde{C}_{z,j0})^2]\, d\omega \tag{5}$$

Now, the unknowns will have to be found by minimizing this error. It is easily observed that

$$M_0 = \frac{\sum_{j=1}^{M} \int_0^\infty [\tilde{\dot{u}}_j \tilde{C}_{x,j0}\, e^{-i\omega\tau_j} + \tilde{\dot{v}}_j \tilde{C}_{y,j0}\, e^{-i\omega\tau_j} + \tilde{\dot{w}}_j \tilde{C}_{z,j0}\, e^{-i\omega\tau_j}]\, d\omega}{\sum_{j=1}^{M} \int_0^\infty [\tilde{C}_{x,j0}^2 + \tilde{C}_{y,j0}^2 + \tilde{C}_{z,j0}^2]\, d\omega} \tag{6}$$

However, there will be difficulties in minimizing the error with respect to $(x_0,y_0,z_0,\phi_0,\delta_0,\lambda_0)$. This can be circumvented by observing that the following compatibility conditions independent of M_0 and τ_j can be obtained for the locational unknowns.

$$\frac{\tilde{\ddot{u}}_j}{\tilde{\ddot{v}}_j} = \frac{\tilde{C}_{x,j0}}{\tilde{C}_{y,j0}}; \quad \frac{\tilde{\ddot{v}}_j}{\tilde{\ddot{w}}_j} = \frac{\tilde{C}_{y,j0}}{\tilde{C}_{z,j0}}; \quad \frac{\tilde{\ddot{w}}_j}{\tilde{\ddot{u}}_j} = \frac{\tilde{C}_{z,j0}}{\tilde{C}_{x,j0}} \qquad (7)$$

These conditions lead to another mean square error expressed as

$$E^2 = \sum_{j=1}^{M} \int_0^{\infty} [(\tilde{\ddot{u}}_j \tilde{C}_{y,j0} - \tilde{\ddot{v}}_j \tilde{C}_{x,j0})^2 + (\tilde{\ddot{v}}_j C_{z,j0} - \tilde{\ddot{w}}_j \tilde{C}_{y,j0})^2 + (\tilde{\ddot{w}}_j \tilde{C}_{x,j0} - \tilde{\ddot{u}}_j \tilde{C}_{z,j0})^2]\, d\omega \qquad (8)$$

This expression contains six unknowns $(x_0,y_0,z_0,\phi_0,\delta_0,\lambda_0)$ which can be found out by minimizing this error function. Once these six location coordinates are found, M_0 is known from equation (6) in terms of τ_j (j=1,2,..M). These in turn, are found by minimizing the mean square error in equation (5). These τ_j values are applied on to the records and the whole exercise is repeated till the M_0 and τ_j values converge along with $(x_0,y_0,z_0,\phi_0,\delta_0,\lambda_0)$. Since this exercise is essential for San Fernando and Uttarakashi events, it would be interesting to compare the results of this approach with a case where the time instants are known. For this purpose the Imperial Valley data comes in handy, since the absolute trigger times are known for several stations [11]. In Figure 2 the station distribution for this event is shown. The velocity model [11] used for the region is presented in Table 1. The convergence of the trigger times τ_j and a comparison with the observed values is presented in Table 2. It is noted that the procedure for finding τ_j and the focal point converges in about four steps. The value of M_0 obtained is equal to 5.4×10^{18} Nm, which matches with the reported value of 6×10^{18} Nm [11]. The τ_j values also compare with recorded values in many cases. The differences with some stations are attributed to the near source regional model that can only be approximate. It is found that for the Chi-Chi array data, the comparison is much better.

Table 1. Near Source Regional Model (Imperial Valley Earthquake)

Layer No.	Thickness (km)	V_P (km/s)	Q_p	V_s (km/s)	Q_s	Density
1	0.8	1.9	100	0.8	80	1.8
2	0.8	2.5	100	1.2	80	2.9
3	0.8	3.1	100	1.5	80	2.1
4	0.8	3.6	100	1.9	80	2.2
5	0.8	4.2	100	2.3	80	2.3
6	0.8	4.8	200	2.6	120	2.4
7	0.8	5.4	200	2.9	120	2.5
8	5.5	5.5	200	3.0	120	2.5
9	0.5	5.6	200	3.1	120	3.0
10	∞	7.2	200	4.2	120	2.8

Table 2. Consistent Trigger Times of SMA Data
(Imperial Valley Earthquake)

STATION	Iteration (τ_j)				T_r-T_0 Observed
	1	2	3	4	
EMO	5.43	5.58	5.54	5.54	5.3
AGR	2.65	2.84	2.87	2.87	2.48
BCR	2.86	2.82	2.81	2.81	2.71
HVP	5.68	5.95	5.96	5.97	NA
CXO	4.69	4.78	4.79	4.79	4.47
E01	9.75	9.84	9.87	9.87	7.84
E04	7.34	7.52	7.58	7.59	7.38
E05	6.73	6.65	6.65	6.65	6.99
E06	7.89	7.49	7.48	7.49	7.00
E07	7.34	7.46	7.48	7.48	NA
ICC	7.89	7.65	7.67	7.67	NA
BRA	10.45	10.35	10.36	10.36	9.14
SUP	14.72	14.81	14.89	14.89	NA
CPO	4.34	4.72	4.71	4.71	4.44

T_r - Triggering Time, T_0 - Origin Time of Earthquake

SOURCE MAPPING

The above analysis helps to align the SMA records consistently at their starting point and to find (x_0,y_0,z_0) the most likely point for initiation of rupture. It remains to find the details of the spatial distribution of the forces around this location. For this purpose, the forces causing the ground motion are modeled as a sequence of double couples applied with a time lag of Δt seconds. Since it is reasonable to take the duration of the earthquake as equal to the duration of strong motion (T), the number of unknown double couples will be $N=T/\Delta t$. Each such elemental source is defined in terms of a double couple M_n with rise time t_r triggering at an instant $(n-1)\Delta t$, $(n=1,2,\ldots N)$. The point of application and orientation of M_n is characterized in terms of $(x_{sn},y_{sn},z_{sn},\phi_n,\delta_n,\lambda_n)$. These unknowns are again found by minimizing the mean square error between the recorded velocities and their corresponding analytical expressions in the time domain.

$$E^2 = \sum_{j=1}^{M} \int_0^{T_j} \left[\left(\dot{u}_j(t) - \sum_{n=1}^{N} M_n C_{x,jn} \right)^2 + \left(\dot{v}_j(t) - \sum_{n=1}^{N} M_n C_{y,jn} \right)^2 + \left(\dot{w}_j(t) - \sum_{n=1}^{N} M_n C_{z,jn} \right)^2 \right] dt \qquad (9)$$

The total number of unknowns will be 8N where, N depends on Δt and T. Reducing the time interval will increase the number of unknowns but makes the numerical scheme more ill conditioned. By trial, $\Delta t=0.5$ second has been chosen as a reasonable value for carrying out the computations. Since, analytical methods for simulating ground motion are reliable up to 1hz [11] the time interval of 0.5s is considered reasonable. The hybrid global search algorithm as used by Hartzell *et al* [13, 16], which is a combination of simulated annealing and downhill simplex method, is used to find the unknowns with three constraints. The first constraint is that M_n has to be positive. The second constraint is on the locations (x_{sn},y_{sn},z_{sn}) of the double couple M_n. It is prescribed that the distance between successive points cannot exceed the value $V_s\Delta t$; where V_s is the shear wave velocity in the medium. The third constraint is on $(\phi_n,\delta_n,\lambda_n)$. These are taken between two bounds, selected based on teleseismic results, reported in the literature.

NUMERICAL RESULTS

The source geometry and the consistent sequence of double couples have been found for four past earthquakes. In all the cases, the recorded data has been resolved in the NS and EW directions before further analysis. When large number of records is available, as with the Imperial Valley and Chi-Chi events, a few of them have been kept outside the source modeling, for independent comparison with analytical results obtained from the newly mapped source.

Imperial Valley Earthquake (15th October 1979)

This earthquake produced large number of strong motion records and they have been well studied in the literature [10,11,17]. For the present work, data at fourteen stations distributed around the Imperial fault are considered (Figure 2). The strike, dip and rake angles are respectively constrained as ($130^0 < \varphi < 150^0$), ($80^0 < \delta < 90^0$) and ($90^0 < \lambda < 180^0$). The rise time t_r is varied between 0 to 2s. Optimal values of ($x_{sn}, y_{sn}, z_{sn}, \varphi_n, \delta_n, \lambda_n$) which minimize the mean square error provide the rupture surface. The corresponding values of M_n and t_r are presented in Table 3. The rupture source is mapped in Figure 3. The mapped source shows a right lateral strike slip, which is in agreement with field observations and the results of Hartzell [11]. A further check on the efficiency of the present approach is provided by studying how the analytically determined source predicts near source ground motion. Accordingly, velocity time histories at two stations (E03 and E10), not included in source modeling, have been computed. In Figure 4, these analytical results are compared with instrumentally recorded ground response.

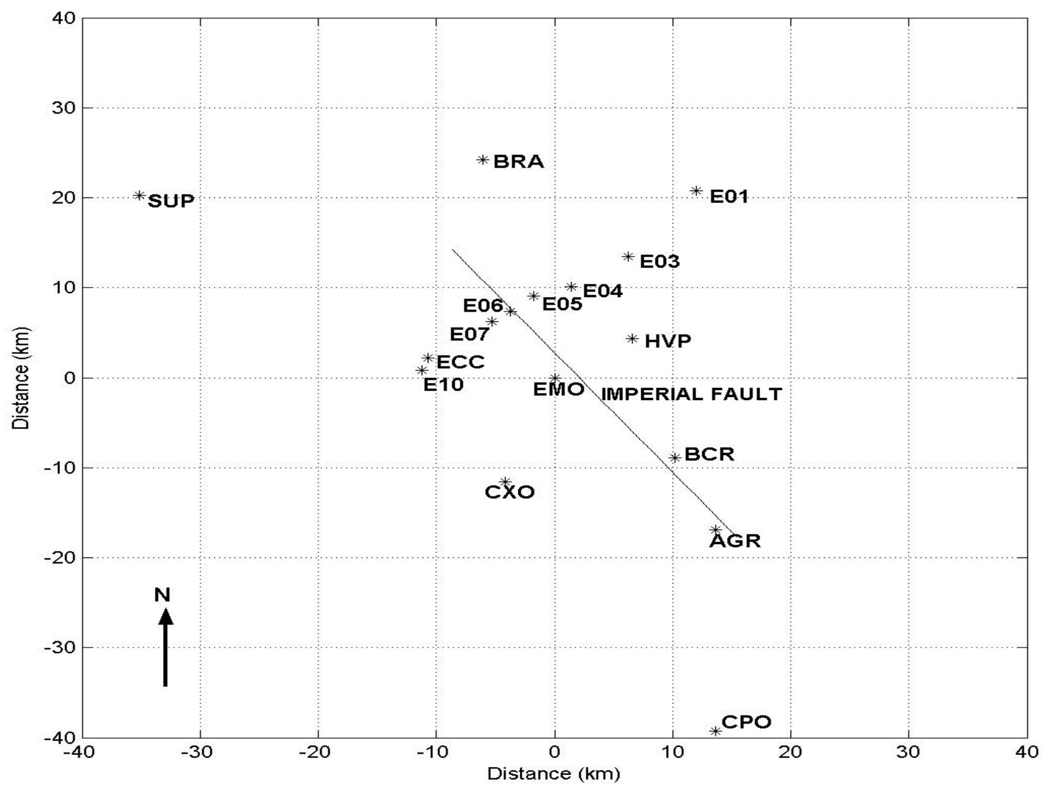

Figure 2. SMA Stations of Imperial Valley Earthquake

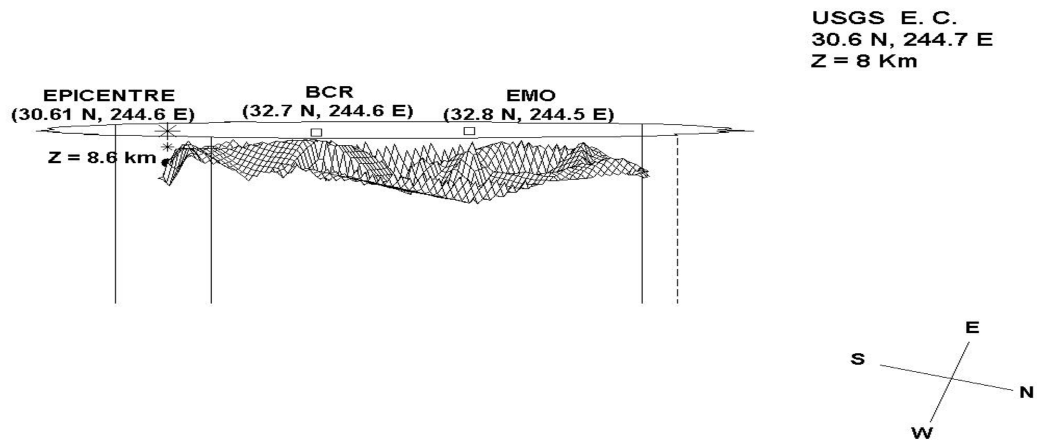

Figure 3. Estimated Rupture Zone of Imperial Valley Earthquake

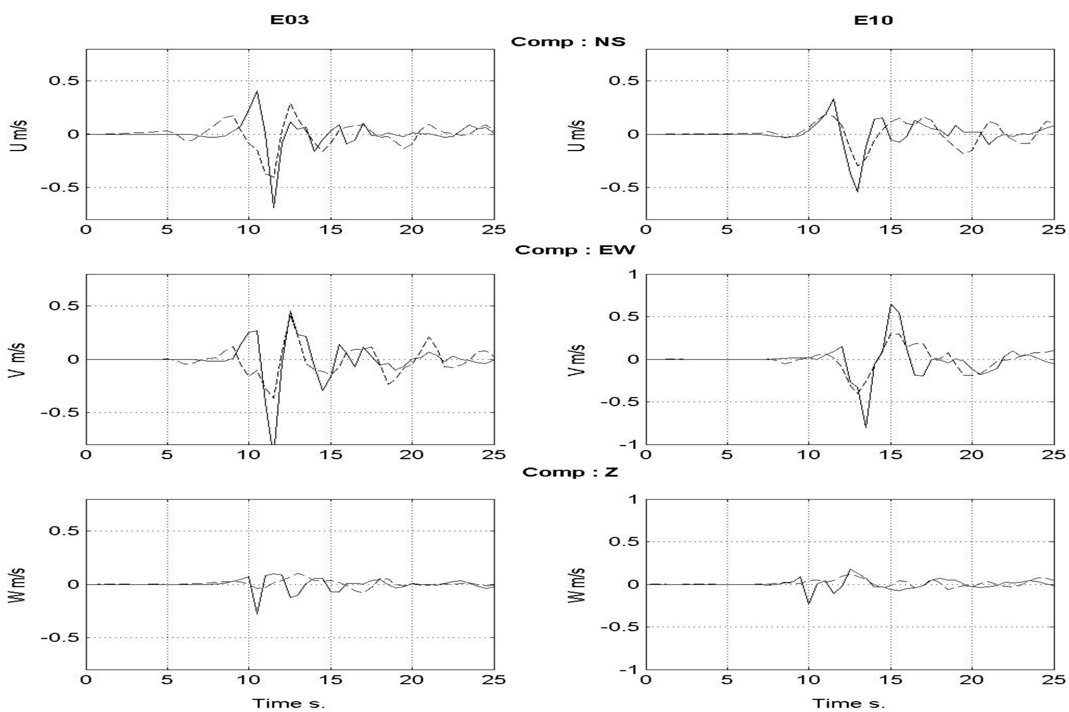

Figure 4. Comparison between Computed and Recorded Response.
———— Recorded ------------ Simulated

Table 3. Points of Application, Orientation and Rise Times of Double Couples M_n (Imperial Valley Earthquake)

S. No.	Time of application of M_n	Point of Application X_{0n} (km)	Y_{0n} (km)	Z_{0n} (km)	Orientation φ_n (deg)	δ_n (deg)	λ_n (deg)	Rise Time t_{rn} (sec)	M_n (10^{17}Nm)
0	0	13.0	-14.2	8.6	142	82	171.6	0.4	0.68
1	0.5	12.9	-14.0	7.1	149	84	168.4	1.5	0.91
2	1.0	11.0	-15.4	7.1	150	83	170.3	0.6	0.95
3	1.5	15.9	-16.1	8.3	139	84	166.6	1.1	2.21
4	2.0	12.0	-14.7	9.6	144	86	168.6	0.3	0.99
5	2.5	17.0	-15.3	9.1	134	84	164.5	1.4	6.98
6	3.0	12.9	-13.3	1.4	132	88	171.5	0.7	0.22
7	3.5	11.9	-14.6	5.6	152	88	175.2	1.7	0.73
8	4.0	14.0	-19.1	9.7	143	86	170.5	1.7	4.96
9	4.5	11.9	-13.2	4.7	133	82	172.8	1.2	0.82
10	5.0	17.0	-17.7	6.2	146	87	164.1	0.9	1.12
11	5.5	11.0	-13.8	4.5	147	86	167.5	1.8	1.79
12	6.0	11.0	-14.1	3.4	139	82	175.6	1.6	1.90
13	6.5	4.0	-6.3	3.4	133	90	173.6	1.3	1.07
14	7.0	2.9	-1.6	9.2	144	90	169.2	1.6	3.98
15	7.5	13.9	-19.3	8.7	131	86	171.3	1.3	0.70
16	8.0	14.0	-16.3	10.7	148	90	175.8	0.7	3.27
17	8.5	7.0	-7.4	4.5	150	90	161.1	0.6	1.01
18	9.0	3.9	-0.8	3.5	149	90	172.0	0.7	1.06
19	9.5	16.0	-15.3	10.5	137	90	161.0	1.1	0.38
20	10.0	16.5	-18.4	1.2	133	88	168.3	1.4	0.42
21	10.5	-1.2	1.6	2.5	141	80	166.1	0.6	1.35
22	11.0	10.0	-9.3	7.7	149	90	177.4	1.7	1.10
23	11.5	-2.5	3.6	8.9	150	86	160.3	1.1	3.45
24	12.0	1.9	-3.3	8.3	134	84	175.3	0.7	0.25
25	12.5	14.7	-15.4	2.3	148	90	179.4	1.4	0.01
26	13.0	0.6	8.7	10.8	135	90	179.8	1.1	6.34
27	13.5	3.0	-4.3	4.3	143	82	175.7	0.9	0.90
28	14.0	9.7	-9.3	4.8	134	86	168.7	1.4	0.45
29	14.5	-1.3	-1.3	1.9	145	86	169.9	1.2	0.58
30	15.0	16.5	-19.4	4.3	142	86	164.2	1.6	0.27
31	15.5	-3.8	2.6	9.3	144	87	172.8	1.9	2.49
32	16.0	-1.1	2.6	5.1	143	88	166.4	1.0	1.01
33	16.5	0.1	7.7	2.1	148	87	179.2	1.8	0.27
34	17.0	-2.0	6.6	5.6	158	93	174.5	0.3	0.26
35	17.5	6.9	-9.3	3.2	139	87	168.2	1.9	0.35
36	18.0	2.3	-3.3	0.8	145	92	174.8	0.5	0.27
37	18.5	-1.0	10.6	6.2	143	68	165.3	0.5	0.24
38	19.0	-0.3	6.6	1.2	137	80	168.7	1.8	0.42
39	19.5	6.1	-0.3	8.9	141	88	178.6	1.5	2.23
40	20.0	1.2	-3.3	8.4	131	84	173.6	0.3	0.61
41	20.5	-4.5	4.6	10.4	143	83	164.2	0.1	0.48
42	21.0	1.1	1.7	10.3	138	89	176.7	1.8	0.66
43	21.5	1.8	-3.4	10.4	142	94	172.5	0.4	0.73
44	22.0	13.2	-13.3	2.4	136	82	162.6	0.6	0.09
45	22.5	-1.0	2.6	6.6	141	85	164.1	1.3	0.35
46	23.0	-6.8	9.9	0.5	139	82	172.1	0.6	0.05
47	23.5	15.8	-18.2	4.1	138	81	172.5	0.9	0.08
48	24.0	-5.2	8.6	1.5	144	85	167.4	0.1	0.02
49	24.5	-1.4	9.6	9.8	140	89	171.5	1.9	0.04

San Fernando Earthquake (9th February 1971)

The regional geology and seismological details of the event are well documented [9,18]. For the present work, data at eleven stations have been considered. The velocity model of the region is taken from Langston [18]. The strike, dip and rake angles are constrained as ($270^0<\varphi<290^0$), ($30^0<\delta<60^0$) and ($0^0<\lambda<90^0$). The strong motion data is first adjusted for starting times before estimating the detailed source as described previously. The estimated source is mapped in Figure 5. The rupture surface reaches a depth of 100 meters below the surface at a distance of 10 km from Pacoima dam. This correlates with observed surface ruptures in this region as reported by Heaton [19]. He has also identified San Fernando earthquake to be a double event occurring on two different faults. The source geometry of Figure 5 shows a sharp change in its orientation, supportive of the results of Heaton [19].

Uttarakashi Earthquake (20th October 1991)

The strong motion records of this event have been taken from the study of Chandrasekaran and Das [20]. The velocity model of the region is the one given by Khattri *et al* [21]. The strike, dip and rake are constrained as ($270^0<\varphi<320^0$), ($10^0<\delta<20^0$) and ($80^0<\lambda<120^0$). In Figure 6, the source geometry as per the present method using data at five stations is shown. The source parameters obtained here compare well with those reported by India Meteorology Department (IMD). The estimated total seismic moment of the event is 7.23 x 10^{18} Nm. The average dip and strike of the fault are found to be 15^0 N and 280^0 E respectively.

Chi-Chi Earthquake (20th September 1999)

This event is well recorded on large number of modern digital instruments. The strong motion data was obtained from the Central Weather Bureau of Taiwan [Lee *et al* 22]. Eighteen strong motion station data within a distance of 50 km from the Chelungpu fault are used for mapping the source geometry. The velocity model for the region is taken from Ma *et al* [23]. The geometrical constraints used are ($0^0<\varphi<10^0$), ($20^0<\delta<40^0$) and ($0^0<\lambda<90^0$). The rupture surface estimated by the present method is shown in Figure 7. The upper part of the rupture boundary approaches the surface, consistent with field observations of ground uplift. The total seismic moment M_0 of this event is estimated as 3.3 x 10^{20} Nm. In Table 4, the mean values of the parameters of the computed random source model for all the four earthquakes are compared with values reported in the literature. It is seen that the approach developed here can accurately estimate the overall focal parameters as well as the details of the source consistent with strong motion records.

Table 4. Parameters of the Random Source Model

Event	Imperial Valley		San Fernando		Uttarakashi		Chi – Chi	
	USGS*	Authors	USGS*	Authors	USGS*	Authors	CWB**	Authors
Epicentre Lat. ^{0} N Long. ^{0} E	 30.6 244.7	 30.61 244.6	 34.41 241.4	 34.4 241.6	 30.78 78.77	 30.6 78.2	 23.85 120.81	 23.86 120.3
Depth. km	8	8.6	13	14.3	10	19	7	19.4
Dip (δ)	90^0	85^0	45^0	44^0	14^0	18^0	29^0	33^0
Strike (φ)	143^0	140^0	288^0	282^0	317^0	284^0	3^0	4^0
Rake (λ)	180^0	170^0	172^0	175^0	114^0	103^0	130^0	143^0
M_o. Nm	6x10^{18}	6.4x10^{18}	1.5x10^{19}	0.33x10^{19}	1.2x10^{19}	0.72x10^{19}	4.6x10^{20}	3.3x10^{20}

* United States Geological Survey, ** Central Weather Bureau of Taiwan.

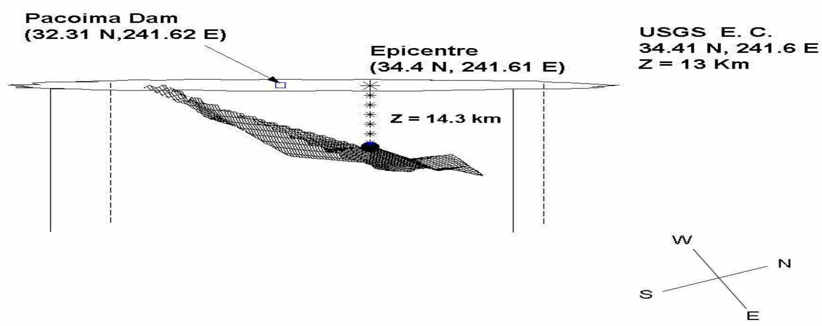

Figure 5. Estimated Rupture Zone of San Fernando Earthquake

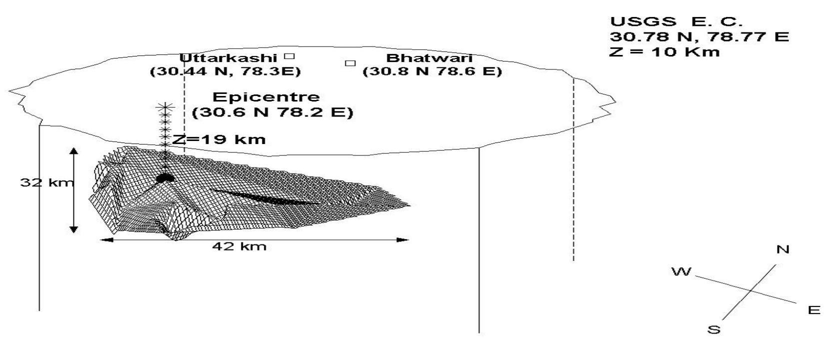

Figure 6. Estimated Rupture Zone of Uttarkashi Earthquake

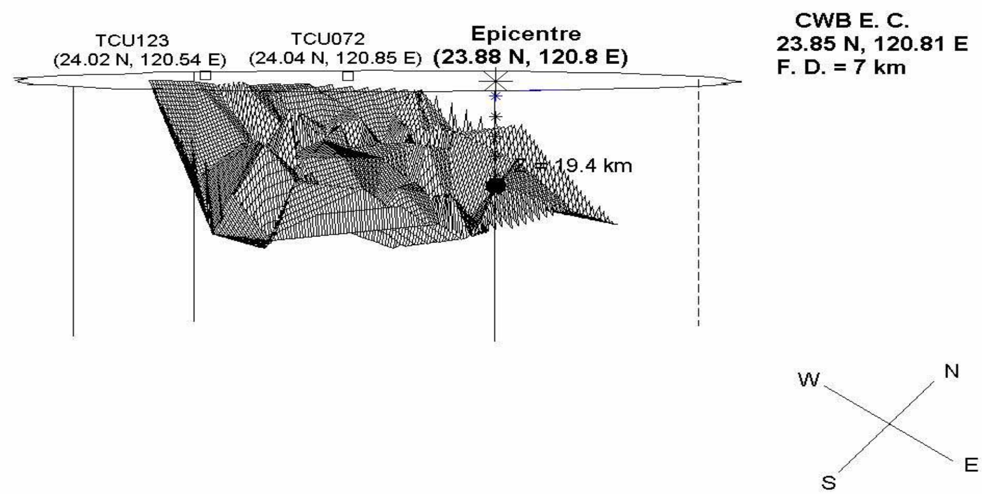

Figure 7. Estimated Rupture Zone of Chi-Chi Earthquake

CONCLUSION

A novel approach to determine the magnitude and location of forces compatible with strong motion records has been developed in this paper. The ground motion during an earthquake is thought to be the response of the near source region, modeled as layered elastic half-space, to the rupture at the fault level. The forces developed at the source during the rupture are represented by a sequence of double couples, applied at equal intervals of time, at unknown locations inside the half-space. The magnitude, rise time and the point of application of the double couples are found out by minimizing the error between the analytically derived surface level station response and the SMA data. A plot of the locations of the double couples directly provides a picture of the rupture zone, compatible with the recorded strong motion. Numerical results are provided for four recorded earthquakes. These are the San Fernando (9.2.1971), Imperial Valley (15.10.1979), Uttarakashi (20.10.1991) and Chi-Chi (20.9.1999) earthquakes. In all the four cases, the present results are consistent with those available in the literature. The major thrust of the present investigation has been to delineate the spatial variability of the double couples, which in turn will help in developing a stochastic source model for strong earthquakes. The limitation of the method is its current inability to handle high frequencies beyond about 5 hz. It is foreseen that with some further improvement, the proposed method will be useful in foreshadowing strong ground motion occurring in thickly populated cities, located near known active faults.

REFERENCES

1. USNRC. "Identification and characterization of seismic sources and determination of safe shutdown earthquake ground motion", Regulatory guide 1.165. 1997.
2. Aki K. "Seismic Displacement Near a Fault". Journal of Geophysical Research 1968; 73: 5359-5376.
3. Haskell NA. "Elastic Displacements in the Near-field of a Propagating Fault". Bulletin of the Seismological Society of America 1969; 59: 865-908.
4. Bouchon M. "Discrete wave number representation of elastic wave fields in three-space dimensions". Journal of Geophysical research 1979; 84(7): 3609-3614.
5. Bouchon M. "A simple Method to calculate Green's functions for elastic layered media". Bulletin of the Seismological Society of America 1981; 71: 959-971.
6. Deodatis G, Shinozuka M. and Papageorgiou A. "Stochastic wave representation of seismic ground motion. I: F-K spectra". J. Engrg. Mech., ASCE 1990; 116: 2363-2379.
7. Zhang R, Yong Y, Lin YK. "Earthquake ground motion modeling. I: Deterministic point source". J. Engrg. Mech., ASCE 1991; 117: 2114-2132.
8. Aki K. and Richards PG. "Quantitative Seismology: Theory and Methods". Vol. 1, WH. Freeman, New York, 1980.
9. Trifunac, MD, "A three-dimension model for the San Fernando, California, earthquake of February 9,1971". Bulletin of the Seismological Society of America 1974; 64: 149-172.
10. Olson AH, Apsel RJ. "Finite faults and inverse theory with applications to the 1979 Imperial Valley earthquake". Bulletin of the Seismological Society of America 1982; 72(6): 1969-2001.
11. Hartzell S, Heaton T. "Inversion of strong ground motion and teleseismic waveform data for the fault rupture history of the 1979 Imperial Valley, California, earthquake". Bulletin of the Seismological Society of America 1983; 73: 1553-1583.
12. Cotton F, Campillo M. "Frequency domain inversion of strong motions: application to the 1992 Landers earthquake". Journal of Geophysical Research 1995; B3: 3961-3975.
13. Hartzell S, Liu P, Mendoza C. "The 1994 Northridge, California, earthquake: investigation of rupture velocity, risetime, and high-frequency radiation". Journal of Geophysical Research 1996; 101, B9: 20091- 20108.
14. Das S, Suhadolc P. "On the inverse problem for earthquake rupture. The Haskell-type source model". Journal of Geophysical Research 1996;101: 5725-5738.
15. Iyengar RN, Agrawal SK. "Earthquake source model using strong motion displacement as response of finite elastic media". Proc. Indian Acad. Sci.(Earth Plant. Sci.) 2001; 110(1): 9-23
16. Hartzell S, Liu P. "Determination of Earthquake Source Parameters Using a Hybrid Global Search Algorithm". Bulletin of the Seismological Society of America 1995; 85(2): 516-524.
17. Trifunac MD, Jordanovski LR. "Least Square Inversion with Time Shift Optimization and an Application to Earthquake Source Mechanism". Soil Dynamics and Earthquake Engineering 1990; 9(5): 243-254.
18. Langston CA. "The February 9, 1971 San Fernando Earthquake: A study of source finite-ness in Teleseismic Body Waves". Bulletin of the Seismological Society of America 1978; 68(1): 1-29.
19. Heaton TH. "The 1971 San Fernando earthquake: a double event ?". Bulletin of the Seismological Society of America 1982; 72: 2037-2062.
20. Chandrasekaran AR, Das JD. "Strong motion records from Uttarkashi earthquake". Mem. Geol. Soc. India 1995; 30: 133-147.
21. Khattri KN. *et al*. "Seismic Hazard Estimation Using Modeling of Earthquake Strong ground Motions: A brief Analysis of 1991 Uttarkashi Earthquake, Himalaya and Prognostication for a Great Earthquake in the region", Current Science 1994;67(5): 343-353.
22. Lee WHK. *et al* ."CWB free-field strong-motion data from the 21 September Chi-Chi, earthquake: Volume 1. Digital acceleration files on CD-ROM, pre-publication Version (December 6, 1999)". Seismology center, Central Weather Bureau 1999; Taipei, Taiwan.
23. Ma Kuo-Fong *et al.* "Spatial and temporal distribution of slip for the 1999 Chi-Chi, Taiwan, earthquake" Bulletin of the Seismological Society of America 2001; 91(5): 1069-1087.